

Available online at www.sciencedirect.com

Procedia Engineering 10 (2011) 2256–2261

Engineering
Procedia

ICM11

Hyperelastic modelling of post-buckling response in single wall carbon nanotubes under axial compression

Saavedra Flores E. I. ^{a*}, Adhikari, S. ^a, Friswell, M. I. ^a, Scarpa, F. ^b^aCollege of Engineering, Swansea University, Singleton Park, Swansea, SA2 8PP, United Kingdom.^bDepartment of Aerospace Engineering, University of Bristol, Queens Building, University Walk, Bristol, BS8 1TR, United Kingdom.

Abstract

This paper presents a hyperelastic finite element-based lattice approach for the description of post-buckling response in single wall carbon nanotubes (SWCNTs). A one-term incompressible Ogden-type hyperelastic model is adopted to describe the mechanical response of SWCNTs under axial compression. Numerical experiments are carried out and the results are compared to atomistic simulations, demonstrating the predictive capabilities of the present model in capturing post-buckling behaviour and the main deformation mechanisms under large compressive deformations.

© 2011 Published by Elsevier Ltd. Open access under [CC BY-NC-ND license](http://creativecommons.org/licenses/by-nc-nd/3.0/).
Selection and peer-review under responsibility of ICM11

Keywords: Buckling; Single wall carbon nanotube; Hyperelasticity; Finite element method

1. Introduction

Over the last few years, the investigation of carbon nanotubes by means of computational simulations has brought substantial progress, particularly in relation to the understanding of their mechanical behaviour [1, 2, 3]. In the context of numerical models, two main categories can be found extensively in the current literature. The first category corresponds to the atomistic approach [4, 1, 5, 6, 3], in which classical molecular dynamics and tight-binding molecular dynamics constitute the most popular techniques. Although these strategies have been demonstrated to be successful in capturing complex deformation mechanisms in atomistic systems, they suffer from the drawback of excessive computing costs and therefore, their use has been limited to the analysis of small to moderate size problems. The

* Corresponding author. Tel.: + 44 (0) 1792 513177; fax: + 44 (0) 1792 295157.
E-mail address: e.i.saavedra-flores@swansea.ac.uk

second category is represented by finite elements simulations [7, 8, 9, 2, 10, 11]. Particularly in this category, the lattice approach [2, 12] has been demonstrated to be a suitable technique for the analysis of carbon nanotubes. This approach establishes a linkage between structural and molecular mechanics at the C-C bond level, and provides a way to model the deformation of carbon nanotubes by means of conventional finite element analyses using classical beam elements. Curiously, despite the extensive work carried out in this context, a review of the current literature on the finite element-based lattice approach shows that the adoption of a hyperelastic framework to describe the atomic covalent bonds in SWCNTs at large strains continues to be largely ignored. Moreover, the little research reported in this context [13, 14] has been restricted exclusively to the study of carbon nanotubes under axial tension.

In an attempt to encourage others researchers in this field to make use of such concepts our main objective in this paper is to adopt a hyperelastic framework in the constitutive modelling of C-C bonds in order to capture the main features of buckling behaviour in SWCNTs under axial compression. We anticipate here that with the use of such a hyperelastic model, the prediction of the main mechanisms of deformation and the post-buckling response under large strains is achieved successfully.

The paper is organised as follows. Section 2 presents the constitutive description of SWCNTs by means of a hyperelastic framework. The validation of the present model is given in Section 3. Finally, Section 4 summarises our conclusions.

2. Hyperelastic description

A generic finite hyperelastic model is characterised by the existence of a strain energy density function, which defines the evolution of the Kirchhoff stress tensor, τ , in terms of the current Eulerian logarithmic strain tensor, ε . The constitutive equation for the Kirchhoff stress tensor is given by [17, 18]

$$\tau = \frac{\partial \Psi}{\partial \varepsilon}. \quad (1)$$

The strain tensor ε can be represented as a function of the *left stretch tensor*, V , by means of the expression $\varepsilon = \ln V$. Furthermore, if the strain energy function Ψ is assumed to be isotropic, it is possible to adopt a representation for V in terms of the principal stretches, λ_i , $i=1..3$. Hence, we can write the constitutive equation for the eigenvalues τ_i of the Kirchhoff stress tensor as

$$\tau_i = \frac{\partial \Psi}{\partial \ln(\lambda_i)}. \quad (2)$$

The particular choice of the strain energy density Ψ is commonly considered to be a matter of mathematical or experimental convenience. Here, due to its simplicity and predictive accuracy for large deformations in conventional materials, an Ogden hyperelastic isotropic material model [19] is chosen for the mechanical modelling of C-C bonds. A one-term incompressible version of the Ogden strain energy density function is adopted, whose expression is given by

$$\Psi = \frac{2\chi}{\alpha^2} \{(\lambda_1)^\alpha + (\lambda_2)^\alpha + (\lambda_3)^\alpha - 3\}, \quad (3)$$

where χ and α are material parameters. These are $\chi = 3.93$ TPa and $\alpha = 2.0$, along with a C-C bond equivalent diameter $d = 0.10$ nm and an actual shear stiffness is $GAs = 141.24$ nN. Further details about the determination of these values can be found in Saavedra Flores et al. [20]. With the choice of the

these values for the material constants, we enable the present hyperelastic model to recover the AMBER bond stretching, angle bending and torsional force constants, in the infinitesimal strains regime. The length of the equilibrium bond length between carbon atoms is considered here as 0.142 nm.

3. Validation of the model

Our purpose in this section is to validate the present hyperelastic model with published data. The commercial software ABAQUS [21] is used in all our computational simulations. Because of the development of local instabilities during the non-linear deformation process, we adopt the automatic stabilisation method provided by ABAQUS in order to capture buckling and post-buckling response. In all the subsequent analyses presented in this paper, we select the two-noded hybrid beam element, type B31H, which includes transverse shear strains (Timoshenko beam theory) in its formulation. In the cases analysed in this section, the Z axis corresponds to the axial (longitudinal) direction of the tube, whereas X and Y correspond to the transverse directions. Zero prescribed displacements are imposed on all the degrees of freedom of the nodes located at one of the ends of the tube, at $Z = 0$. On the opposite end, we apply incremental compressive displacements in the axial.

Figure 1 illustrates the variation of the strain energy per atom and the deformation mechanisms from our finite element simulations during the compression of a (7,7) SWCNT of 6 nm length. Furthermore, the strain energy reported by [25], using Brenner's first [26] and second [27] generation potential, and also the strain energy calculated by [3], for the same geometry, are also presented here. The finite element mesh consists of 686 nodes and 1015 beam elements.

In a first nearly quadratic regime, the results obtained with our simulation and those obtained from [3] and [25], using Brenner's second generation potential, show perfect matching, up to 0.03 strain. Here, the deformation is uniform as shown in inset (a).

As the compressive deformation progresses these curves tend to diverge up to 0.05 strain in which the molecular dynamics simulation from [3] and the atomic-scale finite element model from [25] using Brenner's second generation potential reach the first instant of buckling. In this stage, Yakobson's simulation displays (although not shown here) two identical flattenings perpendicular to each other, non-symmetrically located along the tube axis. The first buckling mechanism in our simulation is found at a later stage, at 0.072 strain, coinciding closely with the second buckling strain reported by Yakobson, at 0.076. At this point, if we compare the morphological patterns in both cases we will observe that they match perfectly. Inset (b) shows two orthogonal views of the first buckling deformation mechanism predicted by our numerical simulation, characterised by a three axial half-waves symmetric configuration with a still straight axis. Furthermore, we observe that despite the little difference detected at about 0.05 strain between the amount of energy reported by Yakobson and our model, at a strain about 0.07 the results predicted by both simulations tend to converge into the same amount of stored energy. On the contrary, despite the fact that Leung's simulations seem to show a similar deformation mechanism (not shown here), the amount of energy reported in both cases, with Brenner's first and second generation potential, is substantially lower.

Further increase of the compressive deformation results in a new mechanism of deformation, represented by a buckling sideways in which the corresponding flattenings serve as hinges. Inset (c) plots this stage (with two perpendicular views) in our finite element simulation, revealing the preservation of only one plane of symmetry after buckling. Yakobson's simulation predicts this critical strain at 0.09. However, our numerical model varies gradually (discontinuity not visible in the curve) but during a transition which occurs at about this level of strain. In any case, we find again a morphological agreement between both methodologies.

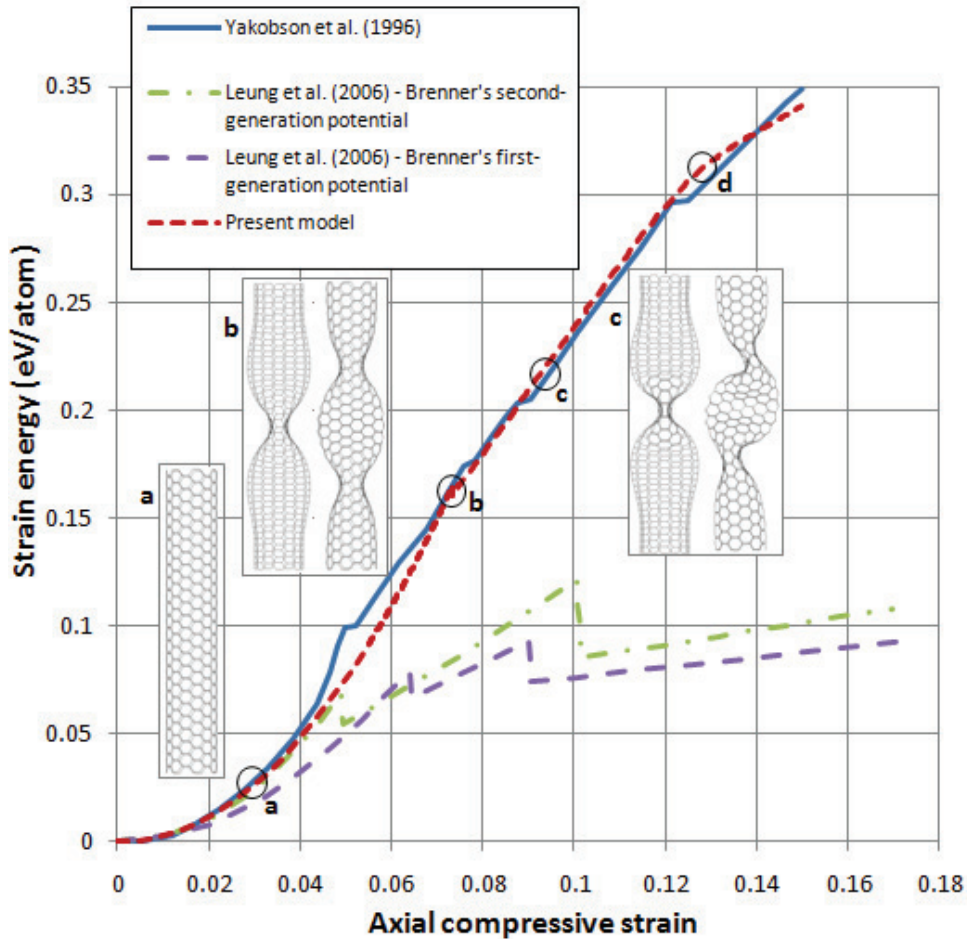


Fig. 1. Strain energy for a (7,7) SWCNT under axial compression.

Moreover, the amount of energy calculated in these two simulations shows almost a perfect match to over 0.12 strain, where a new buckling mechanism is triggered. Yakobson reported over this level of deformation an entirely squashed asymmetric configuration. Our numerical model predicts after 0.125 strain (refer to Figure 1, circle labeled with letter **d**) a morphological pattern (not shown here) similar to that shown in inset (c) but much more distorted. Beyond this point, a gradual transition in the slope of our curve is observed, revealing a slightly lower slope when compared to Yakobson's results. Here, the van der Waals interactions and other different atomic energy terms are crucial in order to describe accurately the mechanical response of carbon nanotubes for even further levels of deformations.

4. Conclusions

The buckling behaviour of single wall carbon nanotubes (SWCNTs) has been investigated by means of a finite element-based lattice approach. A one-term incompressible Ogden-type hyperelastic model has been chosen to describe the mechanical response of SWCNTs under axial compression.

Finite element simulations have been carried out on SWCNT models and the results have been compared to published data, demonstrating the predictive capability of the present hyperelastic model. The proposed description has been able to capture the main deformation mechanisms and post-buckling behaviour under large deformations, revealing the potential applications of our approach on the study of fullerenes.

Acknowledgements

The authors acknowledge funding from the European Research Council through Grant No. 247045 entitled "Optimisation of Multiscale Structures with Applications to Morphing Aircraft".

References

- [1] S. Iijima, C. Brabec, A. Maiti, J. Bernholc, Structural exibility of carbon nanotubes, *Journal of Chemical Physics* 104 (1996) 2089-2092.
- [2] C. Li, T. W. Chou, A structural mechanics approach for the analysis of carbon nanotubes, *International Journal of Solids and Structures* 40 (2003) 2487-2499.
- [3] B. Yakobson, C. Brabec, J. Bernholc, Nanomechanics of carbon tubes: Instabilities beyond linear response, *Physical Review Letters* 76 (1996) 2511-2514.
- [4] E. Hernandez, C. Goze, P. Bernier, A. Rubio, Elastic properties of c and bxcynz composite nanotubes, *Physical Review* 80 (1998) 4502-4505.
- [5] K. M. Liew, C. H. Wong, X. Q. He, M. J. Tan, S. A. Meguid, Nanomechanics of single and multiwalled carbon nanotubes, *Physical review B* 69 (2004) 115429.
- [6] K. Mylvaganam, L. C. Zhang, Important issues in a molecular dynamics simulation for characterising the mechanical properties of carbon nanotubes, *Carbon* 42 (2004) 2025-2032.
- [7] R. Batra, A. Sears, Continuum models of multi-walled carbon nanotubes, *International Journal of Solids and Structures* 44 (2007) 7577-7596.
- [8] X. Chen, C. Cao, A structural mechanics study of single-walled carbon nanotubes generalized from atomistic simulation, *Nanotechnology* 17 (2006) 1004-1015.
- [9] N. Hu, K. Nunoya, D. Pan, T. Okabe, H. Fukunaga, Prediction of buckling characteristics of carbon nanotubes, *International Journal of Solids and Structures* 44 (2007) 6535-6550.
- [10] C. Li, T. W. Chou, Modeling of elastic buckling of carbon nanotubes by molecular structural mechanics approach, *Mechanics of Materials* 36 (2004) 1047-1055.
- [11] K. I. Tserpes, P. Papanikos, Finite element modeling of single-walled carbon nanotubes, *Composites. Part B: engineering* 36 (2005) 468-477.
- [12] F. Scarpa, S. Adhikari, C. Remillat, The bending of single layer graphene sheets: the lattice versus continuum approach, *Nanotechnology* 21 (2010) 125702.
- [13] X. Ling, S. Atluri, A hyperelastic description of single wall carbon nanotubes at moderate strains and temperatures, *Computer Modelling in Engineering and Science* 21 (2007) 81-91.
- [14] E. I. Saavedra Flores, S. Adhikari, M. I. Friswell, F. Scarpa, Hyperelastic finite element model for single wall carbon nanotubes in tension, *Computational Materials Science* 50 (2011) 1083-1087.
- [15] G. Cao, X. Chen, The effects of chirality and boundary conditions on the mechanical properties of single-walled carbon nanotubes, *International Journal of Solids and Structures* 44 (2007) 5447-5465.

- [16] W. D. Cornell, P. Cieplak, C. I. Bayly, I. R. Gould, K. M. Merz, D. M. Ferguson, D. C. Spellmeyer, T. Fox, J. W. Caldwell, P. A. Kollman, A second generation force field for the simulation of proteins, nucleic acids, and organic molecules, *Journal of the American Chemical Society* 117 (19) (1995) 5179-5197.
- [17] E. A. de Souza Neto, D. Peric, D. R. J. Owen, *Computational Methods for Plasticity: Theory and Applications*, Wiley: Chichester, 2008.
- [18] J. Lemaitre, J. L. Chaboche, *Mechanics of Solid Materials*, Cambridge University Press, Cambridge, 1990.
- [19] R. W. Ogden, *Non-linear elastic deformations*, Chichester: Ellis Horwood, 1984.
- [20] E. I. Saavedra Flores, S. Adhikari, M. I. Friswell, F. Scarpa, Lattice hyperelastic finite element approach for axial buckling of single wall carbon nanotubes, *Submitted for publication*.
- [21] ABAQUS, Theory manual. Version 6.4, Hibbit, Karlsson and Sorensen, Inc., Rhode-Island. USA, 2002.
- [22] N. Silvestre, Length dependence of critical measures in single-walled carbon nanotubes, *International Journal of Solids and Structures* 45 (2008) 4902-4920.
- [23] C. F. Corwell, L. T. Wille, Elastic properties of single-walled carbon nanotubes in compression, *Solid State Communications* 101 (1997) 555-558.
- [24] D. Srivastava, M. Menon, K. Cho, Nanoplasticity of single-walled carbon nanotubes under uniaxial compression, *Physical Review Letters* 83 (1999) 2973-2976.
- [25] A. Leung, X. Guo, X. He, H. Jiang, Y. Huang, Postbuckling of carbon nanotubes by atomic-scale finite element, *Journal of Applied Physics* 99 (2006) 124308.
- [26] D. Brenner, Empirical potential for hydrocarbons for use in simulating the chemical vapour deposition of diamond films, *Physical Review B* 42 (1990) 9458-9471.
- [27] D. Brenner, O. Shenderova, J. Harrison, S. Stuart, B. Ni, S. Sinnott, A second-generation reactive empirical bond order (REBO) potential energy expression for hydrocarbons, *Journal of Physics: Condensed Matter* 14 (2002) 783.